

## Biosynthesis and Characterization of AuNPs Produced Using *Termitomyces heimii* Pellets

Sujata Dabolkar & Nandkumar M. Kamat

To cite this article: Sujata Dabolkar & Nandkumar M. Kamat (2024) Biosynthesis and Characterization of AuNPs Produced Using *Termitomyces heimii* Pellets, Geomicrobiology Journal, 41:3, 256-269, DOI: [10.1080/01490451.2024.2312123](https://doi.org/10.1080/01490451.2024.2312123)

To link to this article: <https://doi.org/10.1080/01490451.2024.2312123>



Published online: 07 Feb 2024.



Submit your article to this journal [↗](#)



Article views: 126





View related articles [↗](#)



View Crossmark data [↗](#)



# Biosynthesis and Characterization of AuNPs Produced Using *Termitomyces heimii* Pellets

Sujata Dabolkar  and Nandkumar M. Kamat 

Department of Botany, School of Biological Sciences and Biotechnology, Goa University, Taleigao, India

## ABSTRACT

A green chemistry approach to the synthesis of AuNPs using the pelletized culture of *Termitomyces heimii* has been attempted. The treatment of pellets of *Termitomyces heimii* and chloroauric acid resulted in the formation of AuNPs. These were characterized using various techniques like UV–visible spectroscopy, X-ray diffraction studies (XRD), Energy-dispersive X-ray analysis (EDX), scanning electron microscopy (SEM), atomic force microscopy (AFM), transmission electron microscopy (TEM), zeta potential, dynamic light scattering (DLS), Fourier Transform Infrared Spectrometry (FTIR), and Raman spectroscopy. The results showed the color change of the interaction mixture from light yellow to purple after 25 min. AuNPs showed max absorbance at 530 nm using a UV–visible spectrum, as evident in forming AuNPs. FTIR spectra revealed the presence of functional groups related to peptides, proteins, monosaccharides, and phenolic compounds, which reduced Gold ions. The EDX technique confirmed the formation of AuNPs. XRD results showed that AuNPs have a face-centered cubic (fcc) crystal. The TEM images showed a successful synthesis of triangular nano prisms to nearly spherical and hexagonal with different sizes ranging between 20 and 150 nm.

## ARTICLE HISTORY

Received 28 July 2023  
Accepted 25 January 2024

## KEYWORDS

AuNPs; biosynthesis; characterization; pellets; *Termitomyces heimii*

## Introduction

Nanotechnology deals with the production and stabilization of various types of nanoparticles (NPs). At present, there exists a need to develop eco-friendly processes for the synthesis of NPs. Therefore, the attention of the researchers is shifted from physical and chemical processes toward ‘green’ chemistry and bioprocesses (Bhat et al. 2013). These methods employ plants or microorganisms which are inexpensive, easily available, simple to grow, and safe to handle (Ganesan et al. 2020). Many review articles have been published to describe different ways of biosynthesizing NPs, especially microorganisms (Bhattarai et al. 2018; Gour and Jain 2019; Herizchi et al. 2016; Teimuri-Mofrad et al. 2017; Tepale et al. 2019; Usman et al. 2017). Research demonstrates how diverse group of metal NPs as well as their alloys are biologically blended by bacteria, fungi, actinomycetes, and yeasts (Banerjee and Ravishankar Rai 2018; Barabadi et al. 2014; Das et al. 2010a, 2010b). Preparation of NPs using green chemistry approach is advantageous over physical and chemical methods owing to its environmental significance. In the biological methods, it is found that the extracts of living organisms act both as reducing and capping agents in the synthesizing process of the NPs. The reduction of metal ions in combination with biomolecules found in the extracts of enzymes/proteins, amino acids, polysaccharides, and vitamins is environmentally benign. In this regard rapid and

green synthetic methods using biological extracts have gained more importance in NP synthesis. However, the mechanism of involvement of biomolecules is not well understood till now.

## Mycosynthesis of nanoparticles

Once the microbes are isolated, they can be screened for the production of NPs and further purified for various applications. Among all microorganisms, bacteria and fungi were most often used until now. Researchers isolated *Pseudomonas stutzeri* from silver mines in 1999 which is known to have synthesized AuNPs for the first time in history and there have been many bacteria recognized to produce various metal NPs (Banerjee and Ravishankar Rai 2018). Fungi were found to be more convenient since their biomasses can be easily developed and optimized, biomasses are simpler to handle, cheaper to grow, i.e., they are economically viable, their mycelial mats provide larger surface area for greater wall-binding capacity, produce a comparatively higher quantity of enzymes responsible for diverse processes, help in the comparatively larger scale of production of NPs, have higher bio-accumulation capacity of NPs due to their elevated tolerance level, and their synthesis can be either intra/extracellular but downstream is simpler in this case. Fungal species include different *Aspergillus* spp., *Fusarium* spp., *Verticillium*

spp., and *Trichoderma* spp., and endophytic fungi (Syed et al. 2020) which are known to produce silver, Gold, as well as a variety of other metal NPs.

### Mushrooms in AuNPs synthesis

Only few studies were achieved to reduce Gold ions using isolated fungal compounds from mushrooms like glucan (polysaccharide) from *Pleurotus florida* (Sen et al. 2013), lactase (protein) from *Pleurotus ostreatus* (El-Batal et al. 2015) and *Schizophyllum* from *Schizophyllum commune* (Bae et al. 2007). But most of publications in this field used crude extracts of mushrooms both mycelia and fruiting bodies to synthesize AuNPs (Owaid et al. 2017), such as *Volvariella volvacea* (Philip 2009), *Pleurotus florida* (Bhat et al. 2013), *Pleurotus sapidus* (Sarkar et al. 2013), *Grifola frondosa* (Vetchinkina et al. 2013), *Hericium erinaceus* (Raman et al. 2015), *Pleurotus cornucopiae* var. *citrinopileatus* (Owaid et al. 2017), *Flammulina velutipes* (Narayanan et al. 2015; Rabeea et al. 2020), *Agaricus bisporus* (Eskandari-Nojedehi et al. 2018), and *Lentinula edodes* (Owaid et al. 2019). Table 1 gives the list of mushrooms used in AuNPs synthesis along with their size and shape. Fungi appear to be promising for large-scale production of NPs as these are simpler to grow both in the laboratory and at an industrial scale. Presently, in continuation of the search process of different biological nontoxic and abundantly available species suitable for green synthesis of AuNPs. *Termitomyces heimii* mushroom, a naturally occurring edible mushroom, most dominant in Goa has been considered as a green capping/reducing agent for green synthesis of AuNPs. *Termitomyces heimii* is a species of agaric fungus in the family Lyophyllaceae (Natarajan 1979). Earlier studies has been reported on use of extract of the mushroom for synthesis of AuNPs (Dabolkar and Kamat 2020) and CdS NP (Tudu et al. 2021). In this study we have reported the use of *Termitomyces heimii* culture pellets for large scale production of AuNPs. The study explains a simple, cost-effective eco-friendly method of synthesis of AuNPs

using edible mushroom *Termitomyces heimii*. The treatment of pellets of *Termitomyces heimii* and chloroauric acid resulted in the formation of AuNPs. The green synthesized AuNPs samples were characterized by various comprehensive physical techniques.

### Materials and methods

#### Survey, collection, and taxonomic identification of fruitbodies of *Termitomyces heimii*

Fresh fruitbodies were collected in year 2017–2019 from field and markets of Goa. Collected specimens were identified using standard published keys (Botha and Eicker 1991; Heim 1977; Karun and Sridhar 2013; Morris 1986; Mossebo et al. 2009; Pegler and Vanhaecke 1994; Tibuhwa 2012; Tibuhwa et al. 2010; Vrinda and Pradeep 2009; Wei et al. 2009). *Termitomyces heimii* being the most dominant species and state mushroom of Goa was used for the present investigations. Fresh, healthy specimens of *Termitomyces heimii* were collected from fields of Goa during monsoon season in 2019 and taxonomically identified using standard published *Termitomyces* keys (Natarajan 1979).

#### Pure culture of *Termitomyces heimii*

The fruitbodies obtained were used for culture isolation and screening for NP synthesis. Cultures obtained from a fresh healthy living mushroom fruitbody were cultured by tissue culture method previously described (Stamets and Chilton 1983). Tissue explants of 0.5cm<sup>2</sup> were taken from sterile exposed context tissue and were inoculated in 2% MEA medium with 0.01mg/mL conc. of Nalidixic acid and Neomycin, incubated in dark at 28°C, subcultured on fresh medium and incubated for 2–12 weeks. Colony characters were recorded. Long-term cultures were stored in 10% (v/v) sterile glycerol (4mL) in gamma sterilized cryovials (Tarsons Products Pvt. Ltd., Kolkata, India) and kept at 25°C and

**Table 1.** Biosynthesis of AuNPs using different mushrooms.

Sr. no	Bioreductant	Size	Shape	References
1	<i>Volvariella volvacea</i>	20–150 nm	Triangular nanoprisms, spherical, and hexagonal	Philip (2009)
2	<i>Pleurotus florida</i>	5–15 nm	Triangular nanoprisms to nearly spherical and hexagonal	Sen et al. (2013)
3	<i>Pleurotus cornucopiae</i> var. <i>citrinopileatus</i>	16–100 nm	Spherical	Owaid et al. (2017)
4	<i>Agaricus bisporus</i>	25 nm	Spherical	Eskandari-Nojedehi et al. (2018)
5	<i>Lentinula edodes</i> (shiitake)	72 nm	Triangular, hexagonal, spherical, and irregular shapes	Owaid et al. (2019)
6	<i>Agaricus bisporus</i>	53 nm	Oval, spherical, drum-like, hexagonal, and triangular shapes	Dheyab et al. (2020)
7	<i>Flammulina velutipes</i>	74.32 nm	Triangular, spherical, and irregular shapes	Rabeea et al. (2020)
8	<i>Inonotus obliquus</i>	23 nm	Spherical, triangle, hexagonal, and rod shaped	Lee et al. (2005)
9	<i>Coprinus comatus</i>	Less than 100 nm	Spherical	Naeem et al. (2021)
10	<i>Cordyceps militaris</i>	15–20 nm	Face-center-cubic structure	Ji et al. (2019)
11	<i>Lignosus rhinocerotis</i>	50–83 nm	Spherical	Katas et al. (2019)
12	<i>Ganoderma applanatum</i>	18.70 nm	Face-centered cubic	Abdul-Hadi et al. (2020)
13	<i>Morchella esculenta</i>	20–150 nm	Spherical and hexagonal	Acay (2021)
14	<i>Pleurotus ostreatus</i> , <i>Lentinus edodes</i> , <i>Ganoderma lucidum</i> , and <i>Grifola frondosa</i>	2–20 nm	Spherical	Vetchinkina et al. (2017)
15	<i>Termitomyces heimii</i>	5–100 nm	Spherical, triangular, and hexagonal	Dabolkar and Kamat (2020)

were checked at 3–4 months interval for viability. All chemicals used for media preparation were obtained from HiMedia Laboratories, Mumbai, India.

### **Pellet production**

Morphologically stable *Termitomyces heimii* cultures were grown on Czapek Dox Agar (CDA) containing 5% sucrose (Carbon source), 0.2% sodium nitrate (Nitrogen Source), 0.1% dipotassium phosphate, 0.05% magnesium sulfate heptahydrate, 0.05% potassium chloride, 0.001% ferrous sulfate heptahydrate, pH 5.5, incubation Temp. 28°C in dark for 6 d. Ten cultural plugs (5 mm diam.) from peripheral growth zone of 6 days old culture were inoculated for cultivation under submerged condition in 100 mL Czapek dox solution with 5 g/L Sucrose as carbon source, in 250 mL flasks and were kept on optical shaker at 150 rpm at 28°C, dark for 6 d. Mycelial suspensions were prepared (Kalisz et al. 1986) centrifuging liquid cultures on a research centrifuge (5000 rpm, 20 min) in sterile centrifuge tubes. The supernatant was decanted, the pellets rinsed with sterile distilled water and resuspended in approximately the same volume of distilled water, containing about 100 glass beads (4.5–5.5 mm diameter). The suspensions were shaken in an orbital shaker (300 rpm, 20 min) to provide fragmented mycelial suspensions. Inoculum was added (1% v/v) in 100 mL of modified Czapek Dox liquid medium and kept on shaker at 150 rpm and incubated at 28°C, in dark for 20 d.

### **Harvesting pellets**

After 20 d of incubation final pH of each flask was determined (Elico, Water Quality Analyzer, PE138, Hyderabad, India) and then the pellets were transferred aseptically to sterile Petri plates in laminar air flow using sterile stainless-steel mesh with pore size 100 µm. Pellets were repeatedly washed three times with sterile distilled water to remove any debris or traces of culture filtrate.

### **Testing of the pellets for AuNPs production**

Five grams (fresh weight) of fungal pellets were exposed to 50 mL of a sterilized aqueous solution of 200 µL (one mM) HAuCl<sub>4</sub> concentrations in 250 mL Erlenmeyer flasks and the flasks were placed on a shaker at 200 rpm and incubated at 35°C for 4 d.

## **Characterization of mycosynthesized AuNPs**

### **UV-visible spectroscopy**

The formation of AuNPs was confirmed by UV-visible spectrometer. The change in color from pale yellow to a pinkish appearance was indicative of the formation of AuNPs. UV-visible spectroscopy biosynthesis of metal ions was monitored by taking 2 mL aliquots of reaction mixture at different time intervals and centrifuging them at 5000 rpm for 10 min. The centrifuged biomass was washed twice with double

distilled water and biofilms were prepared. The biofilms were dried in an oven at 45°C for 1 h and examined by spectroscopic analysis using Shimadzu UV spectrophotometer (UV-1800) (300–800 nm) at Goa University. The biomass samples showing the desired color change were used for further studies.

### **X-ray diffraction spectroscopy**

The NPs emulsion was oven dried at 40°C for 1 d. The dried sample was collected and examined for the structure and composition using powder X-ray diffraction (XRD) spectroscopy. The data was recorded using Ultimate IV powder Diffractometer, Rigaku Corporation-Japan at 45 kV and 20 mA. The dried sample was scanned in the range of 2 theta with 2/min.

### **Zeta potential**

The zeta potential (surface charge) measurement is an approximation value related to the NPs surface electric charge, which is an indirect description of the physical stability of the synthesized NPs in the mixture solution. Of 2 mL of aliquot was tested for Zeta potential at central sophisticated instrumentation facilities (CSIF) BITS Pilani, Goa Campus. The zeta potential of green synthesized AuNPs was determined at 25°C using DLS (Nanotracs Wave, Microtrac, York, PA). Water was used as dispersant, and measurements were conducted in triplicates.

### **Particle size distribution**

A dynamic light scattering (DLS) particle size analyzer (Nanotracs Wave, Microtrac) was used to assess the mean particle size, the particle size distribution (PSD). DLS technique scatters a laser light beam at the surface of dispersed NPs, which results in the detection of the backscattered light. PDI is a dimensionless value that shows the uniformity of the synthesized NPs. Of 2 mL of aliquot was tested for DLS at CSIF BITS Pilani, Goa Campus.

### **Fourier transmission infrared spectroscopy (FTIR) analysis**

The pelletized biomass was washed with sterile distilled water and dried in an oven maintained at 75°C for 48 h. Dried composite of whole pelletized biomass was macerated using mortar and pestle. Samples of 1 mg were mixed with 100 mg of spectroscopic grade KBr, HiMedia. The FTIR spectra were determined between 4000 and 400 cm<sup>-1</sup> using a Shimadzu IR Spirit following parameter: Spectral resolution 4 cm<sup>-1</sup>, 40 scans min<sup>-1</sup>, encoding interval 1 cm<sup>-1</sup>, Happ-Genzel apodization, and scanning speed 2.8 mm s<sup>-1</sup>.

### **SEM-EDX studies**

The biomass was centrifuged at 1500 rpm for 20 min and washed twice with double distilled water. The pelletized biomass was washed with sterile distilled water and dried in an

oven maintained at 75°C for 48h and were mounted onto carbon-coated copper grid. Micrographs were obtained using Carl-Zeiss scanning Electron Microscope (SEM-EDX) (USIC, Goa University, Taleigao, India) analysis were conducted using acceleration voltages between 15 and 20keV (Falconer et al. 2006).

### **Transmission electron microscopy (TEM)**

Transmission electron microscopy (TEM) was used to evaluate of the synthesized AuNPs morphology. Of 3 mg of sample was dispersed in 3 mL of ethanol, sonicated for 10 min. One drop of suspension was placed onto a grid of carbon-coated copper grid (6 $\mu$ L) and kept for 20sec, and grid was allowed to dry. The analysis was carried out using TECNAI G2 TWIN FEG (Thermo Fisher, Waltham, MA) at 200KV was carried out at central Research facilities IIT Delhi.

### **Atomic force microscopy (AFM)**

The AFM is one kind of scanning probe microscopes (SPM). SPMs are designed to measure local properties, such as height, friction, magnetism, with a probe. To acquire an image, the SPM raster-scans the probe over a small area of the sample, measuring the local property simultaneously. The AFM studies were carried out at CRF IIT Delhi using Asylum Research MFP3D-BIO which is a very versatile atomic force microscope (AFM), suitable for use with a wide range of samples and features a vast array of modes. It has a z-range of 40  $\mu$ m (extended head model) and an x and y movement of up to 90  $\mu$ m in a closed loop scan. The microscope differs from most others available on the market due to using separate piezo for each plane. This allows for the use of nano-position sensors, minimizing hysteresis and creep, whilst also ensuring flat scans. The MFP-3D is able to image conductive, semiconductive and insulating samples in both air and liquid environments. The head can be adjusted to fit a wide range of sample sizes and both top down and bottom-up illumination of samples is possible. Analysis was carried out by placing the drop of the sample on a mica slide. Sample preparation for AFM imaging involved a deposition of NP solution on freshly cleaved mica surface during the NP synthesis. Freshly cleaved quadratic mica sheets (Structure Probe Inc./SPI Supplies, West Chester, PA) with sizes 10 $\times$ 10mm glued to the metal pads were used for the deposition of NP solution.

### **Raman spectrophotometry**

Raman Spectroscopy is a nondestructive chemical analysis technique that provides detailed information (Banerjee and Ravishankar Rai 2018) about chemical structure, phase and polymorphy, crystallinity, and molecular interactions. It is based upon the interaction of light with the chemical bonds within a material. Raman is a light scattering technique, whereby a molecule scatters incident light from a high-intensity laser light source. Most of the scattered light

is at the same wavelength (or color) as the laser source and does not provide useful information this is called Rayleigh Scatter. The Raman spectroscopy was carried out using LAB RAM HR Horiba France at CSIF, BITS Pilani Goa Campus. Spectral Ranged from 200 to 2100 nm and Microscope with three objectives; 5x, 10x, and 100x. Available Lasers 532 nm Nd-YAG laser 100 mW, 633 nm HeNe laser 17 mW, and 785 nm diode laser 100 mW (Basiev et al. 1999; Hendra and Stratton 1969; Long 1977).

### **Multivariate statistical analysis**

These spectra were analyzed for signal processing procedure by smoothing on spectral second derivatives using Savitzky-Golay method with 9 points of window using Origin version 8 (OriginLab Corporation, Northampton, MA) graphing and analysis software (Savitzky and Golay 1964).

## **Results**

We were successful in obtaining the pure culture of the *Termitomyces heimii* (Figure 1(a,b)), and pellets as seen in Figure 1(c). Pellets were used successfully in bioreduction. AuNPs swarms were detected within 12–24h in all treatments and were subsequently visualized under stereomicroscope (Figure 1(d)).

### **UV-visible spectroscopy**

UV-visible spectroscopy involves the absorption of light by molecules in the UV-visible region and can be used to determine the color changes and concentration of the formed NPs solution based on the absorbance (Figure 2(a)). Generally, AuNPs absorb in the visible region of the electromagnetic spectrum at 510–570 nm because of SPR transition. Metal NPs have free electrons, which cause an SPR absorption band because of their combined vibration in resonance with the light wave. An SPR spectrum for AuNPs was obtained at 552 nm, as shown in Figure 2(b).

### **X-ray diffraction spectroscopy (XRD)**

The crystalline nature of prepared AuNPs was confirmed using XRD. The presence of intense peaks corresponding to the (111), (200), (220), and (311) Bragg reflections of Gold (identified in the diffraction pattern) agree with those reported for Gold nanocrystals. The XRD spectrum shows two predominant peaks that agree with Bragg's reflection of AuNPs. Diffraction peaks, which appeared at 31.6°C and 45.4°C corresponded to the (111) and (200) planes, respectively (Figure 3). No extra peak was observed in the diffraction peaks. Four different intense peaks at 2 $\theta$  angle: 38.22, 44.42, 64.71, and 77.62 with Bragg reflections corresponding to (111), (200), (220), and (311) in biomass-associated AuNPs. Alternatively, only a single prominent peak was observed at 2 $\theta$  angle: 38.22 with a Bragg reflection corresponding to (111) in extracellular AuNPs.

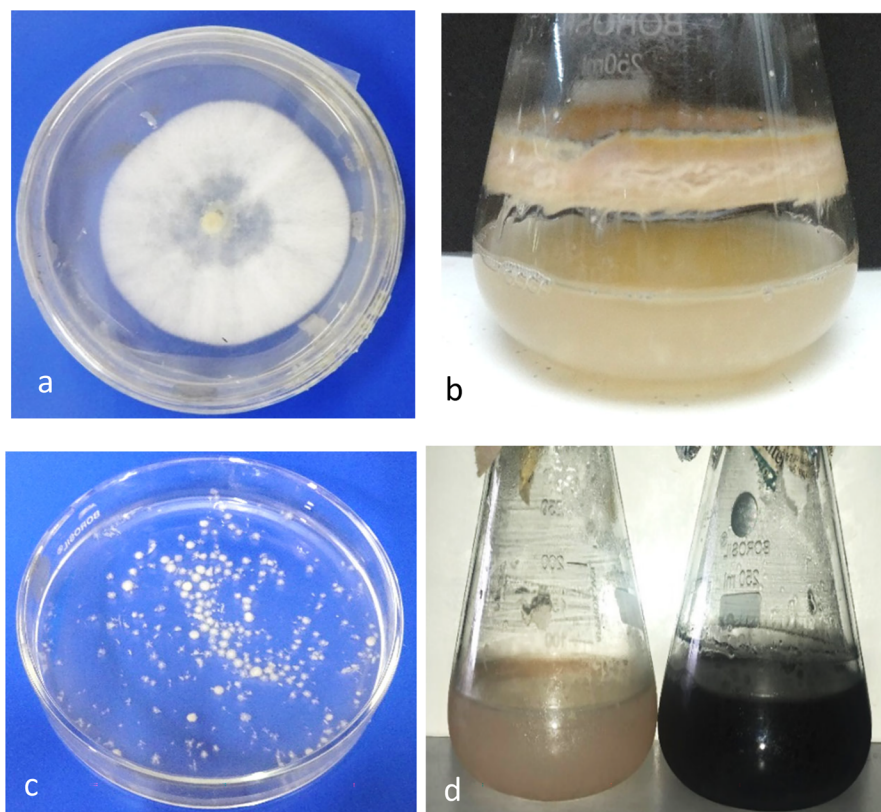


**Figure 1.** (a–d). a,b) 5d old colony of *Termitomyces heimii*; b) Pure culture of the *Termitomyces heimii*; c) Freshly harvested pellets of *Termitomyces heimii*; d) bioreduction shown by pellets.

### Zeta potential and dynamic light scattering

The stability of AuNPs was performed using zeta potential. A zeta value of  $\pm 30$  mV is needed for a suspension to be physically stable while  $\pm 20$  mV is necessary for a combined electrostatic and steric condition. The reading of Au-NPs formed reduced to  $-21.07$  mV. Thus, Au-NPs formed show an acceptable stability with reading not less than the required stable expression (<https://nanocomposix.com/pages/Gold-nanoparticles-physical-properties>) which can be seen in Figure 4(a). DLS is an analytical tool used routinely for measuring the hydrodynamic size of NPs and colloids in a liquid environment and average size was found to be 85 nm which can be seen in Figure 4(b).

### FTIR

The FTIR spectrum of *Termitomyces* pellets is shown in Figure 5(a). Chemically significant regions of FTIR called spectral windows were identified which included fatty acid region dominated by C–H ( $3450$ – $2850$   $\text{cm}^{-1}$ ); amide region dominated by C=O amide I and N–H amide II bands of proteins and peptides ( $1800$ – $1500$   $\text{cm}^{-1}$ ); Mixed region ( $1500$ – $1200$   $\text{cm}^{-1}$ ); polysaccharides region ( $1200$ – $900$   $\text{cm}^{-1}$ ); true finger-printing region ( $900$ – $700$   $\text{cm}^{-1}$ ). As clearly observed in the spectrum, several absorption peaks were centered at 607, 1073, 1299, 1392, 1547, 1632, 2925, and 3271  $\text{cm}^{-1}$ . The AuNPs synthesized by pellets of *Termitomyces* mushroom and chloroauric acid were subjected to FTIR analysis to identify the biomolecules involved in stabilizing the NPs in solution.

As seen in Figure 5(b), the absorption peak centered at  $1070$   $\text{cm}^{-1}$  referred to the C–O stretch vibration, which could be related to the Ester linkages,  $\beta$  (1 $\rightarrow$ 3) glucan, cell wall polysaccharide. Wave number  $1315$   $\text{cm}^{-1}$  was corresponded to the O–H bending polysaccharide, Amide III. The wave number of  $1424$   $\text{cm}^{-1}$  was corresponded to the O–H bending polysaccharide. The intense peak at  $1547$   $\text{cm}^{-1}$  was related to N–H bending – Amide II, chitosan. The peak at  $1652$   $\text{cm}^{-1}$  was related to Amide I, which was created because of the vibrations of carbonyl stretch bonded to the protein. It seems that the proteins have binding ability with Au ions, which in turn creates a surrounded layer on the AuNPs and acts as a capping agent to decrease AuNP agglomeration and increases their stability in the medium. The AuNPs synthesized  $2916$   $\text{cm}^{-1}$  represents CH<sub>3</sub>, CH<sub>2</sub> stretching and peak at  $3271$   $\text{cm}^{-1}$  represents O–H stretching vibration of hydroxyl groups, Amine N–H stretching. Additionally, the bands at  $3400$   $\text{cm}^{-1}$  can be assigned to the O–H stretching vibration of hydroxyl groups, and Amine N–H stretching. These bands correspond to the Amide I–III bands of polypeptides/proteins, and are consistent with previous reports.

### Raman spectroscopy

Figure 6 shows the peaks at 1326.23, 1338.99, 1356, and 1363.52  $\text{cm}^{-1}$  which are due to wagging vibration of  $\delta\text{CH}_2$ , twisting vibration of  $\delta\text{CH}_2$  and  $\nu$  C single bond N modes, respectively whereas 1556.16 which are due to  $\nu$  (C–(NO<sub>2</sub>)) and 1577.87  $\text{cm}^{-1}$  due to  $\nu$  (N=N) aliphatic.

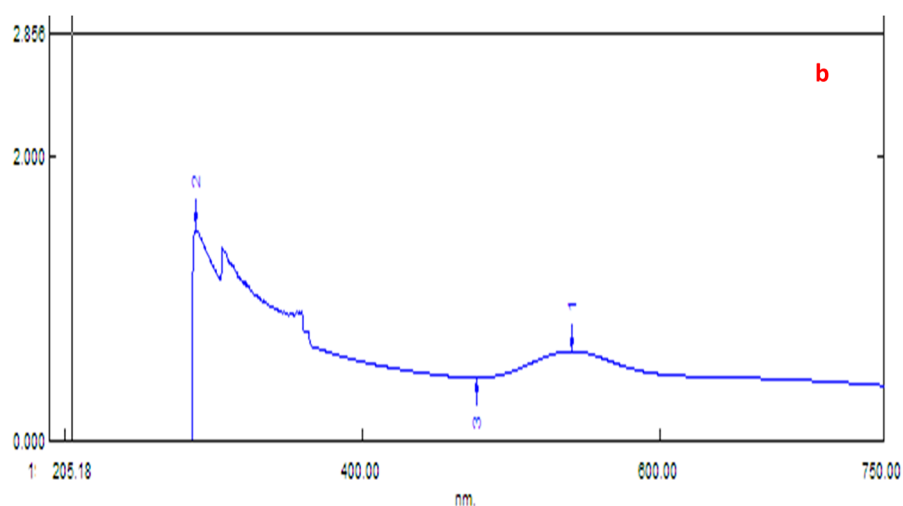


**Figure 2.** (a) UV-visible confirmation of formation of AuNPs and change in the color indicating the formation of AuNPs and (b) UV-visible spectrum for AuNPs was obtained at 552nm.

### SEM-EDX studies

Figure 7(a,b) shows the SEM micrographs of AuNPs in the form of different shapes, such as spheres, hexagons, triangles, rhomboids, and rectangular. SEM demonstrated a polymorphic distribution in size and shapes of AuNPs. Maximum NPs were in the range of 20–50nm. Few NPs were in the range of 50–150 and 150–500nm. Energy-dispersive X-ray spectroscopy (EDX) is an analytical technique that is used for the elemental analysis or chemical characterization. In this study, for verification of AuNPs, EDX spectroscopy analysis was carried out to confirm the presence of elemental Au. The EDX analysis is done to get an indication of the amount of AuNPs present in the biomass. Figure 8 shows presence of Gold.

### Transmission electron microscopy (TEM)

TEM analysis was conducted to evaluate the shape and microstructure of the synthesized AuNPs. A typical TEM

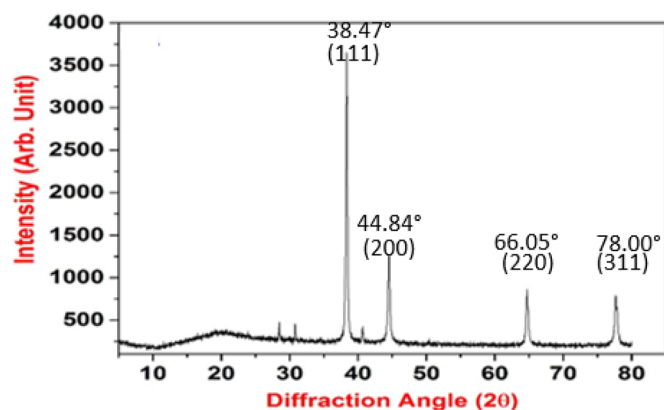


**Figure 3.** XRD patterns of AuNPs.

image of the synthesized AuNPs is shown in Figure 9(a–d). As clearly observed, the synthesized NPs were well dispersed with spherical structures. In fact, spherical NPs were

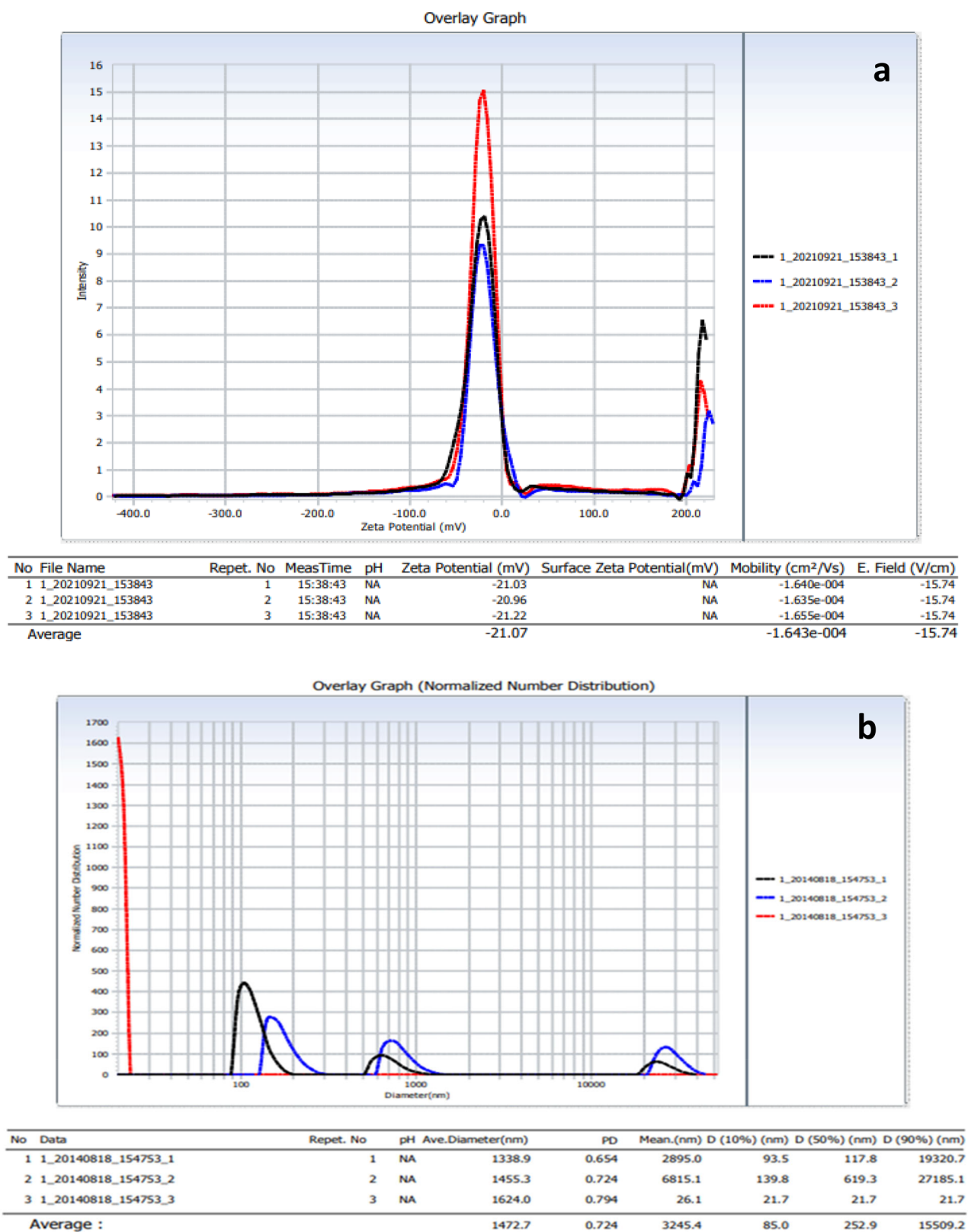
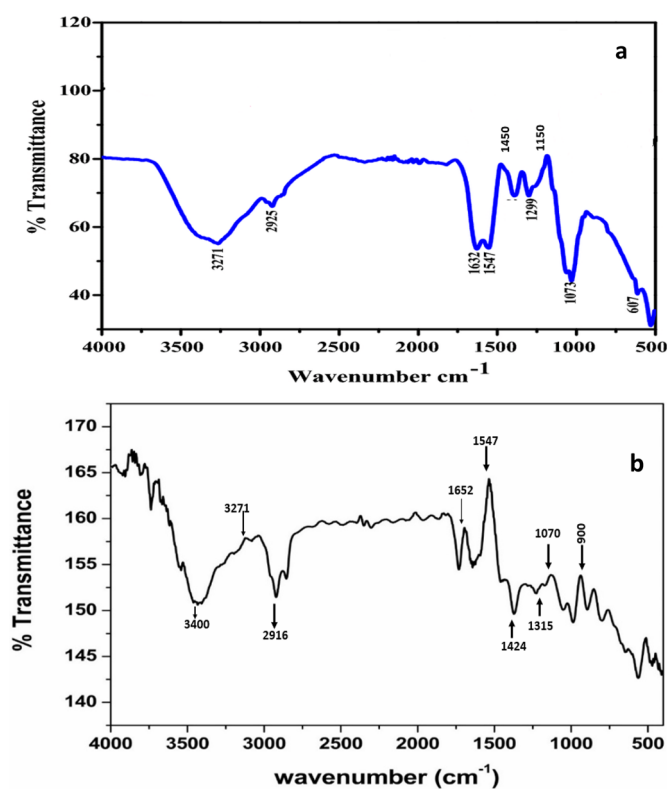


Figure 4. (a) Zeta potential of AuNPs and b) Average particle size (nm).

more abundant than NPs of other shapes. They indicated that the edible mushroom *Termitomyces* pellets can be used to biosynthesize spherical AuNPs with the particle size ranging from 10 to 50 nm. The TEM images showed a

successful synthesis of triangular nano prisms to nearly spherical and hexagonal with different sizes between 20 and 150 nm. The produced NPs were 23.2 nm in size and were mostly spherical in shape.





**Figure 5.** (a) FTIR spectra of *Termitomyces heimii* pellet and spectrum of AuNPs (b).

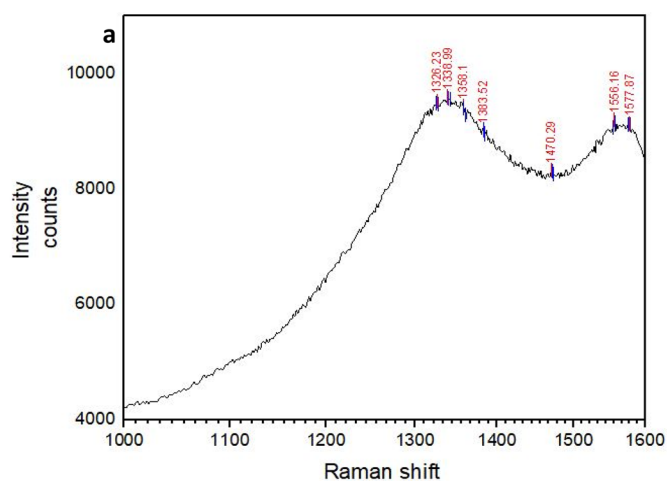


**Figure 6.** Raman spectra of AuNPs.

### Atomic force microscopy (AFM)

A typical example at Figure 10(a–d) is presented AFM images in 2D- and 3D-format, respectively, together with section analysis performed across one of the imaged AuNPs. The small nanoclusters (i.e., NPs with sizes smaller than 5 nm) were easily distinguishable (Figure 10(b)). Figure 10(c) is presented a 3D-image of Gold nanoclusters at the mica surface. These were deposited at the 1 min from the initiation of the synthesis and were determined to have sizes  $1.2 \pm 0.2$  nm. In the next three images the process of NP growing is easily detectable. The performed section analysis

of the individual particles within the time interval of the synthesis showed that the particles sizes span in the range from 1.5 to 20 nm. The histograms of the normalized number of AuNPs obtained from the analysis of about 200 NPs of each of the samples taken (Figure 10(d)).

### Discussion

Fresh and healthy specimens of *Termitomyces heimii*, which is a dominant species in Goa, collected from the fields of Taleigao were taxonomically identified using standard published *Termitomyces* keys (Heim 1942; De Souza and Kamat 2018, De Souza et al. 2018; Singh et al. 2016). We were successful in obtaining the pure culture of the *Termitomyces heimii* (Figure 1(a,b)), obtaining pellets as seen in Figure 1(c) and also successful in use of pellets in bioreduction. Earlier studies have been reported on use of extract of the mushroom for synthesis of AuNPs (Dabolkar and Kamat 2020) and CdS NP (Tudu et al. 2021). AuNPs swarms detected within 12–24 h and in all treatments were subsequently visualized under stereomicroscope. The change in color is a piece of clear evidence for the synthesis of AuNPs from the mushroom due to the behavior of these NPs in the absorption of the UV–visible. This agrees with the results of Owaid et al. (2017), who mycosynthesized AuNPs from the oyster mushroom *Pleurotus cornucopiae*. Moreover, it was found that the highest absorption value of colloidal AuNPs occurred at the wavelength of 530 nm as in UV–visible spectra (Figure 2(b)). The UV–visible spectrum supplied surface plasmon resonance (SPR) phenomenon discovers for Au (Singh et al. 2016). This experiment showed that time was an affirmative act to increase the intensity of the purple color. The spectra exhibit an absorption band around 530 nm, which is a typical plasmon resonance band of Au NPs (Tsutsui et al. 2011). The crystalline nature of as-prepared AuNPs was confirmed using XRD (Figure 3). The presence of intense peaks corresponding to the (111), (200), (220), and (311) Bragg reflections of Gold (identified in the diffraction pattern) agree with those reported for Gold nanocrystals. An estimate of the mean size of the AuNPs formed in the cells was made by using the Debye–Scherrer equation by determining the width of the (111) Bragg reflection (Ahmad et al. 2003, 2005; Nadeem et al. 2017). The XRD spectrum shows two predominant peaks that agree with Bragg’s reflection of AuNPs reported in a previous study. Diffraction peaks, which appeared at 31.6 °C and 45.4 °C corresponded to the (111) and (200) planes, respectively (Figure 3). No extra peak was observed in the diffraction peaks, which indicates that the as-prepared AuNPs were highly purified without any contamination. Earlier studies observed four different intense peaks at  $2\theta$  angle: 38.22, 44.42, 64.71, and 77.62 with Bragg reflections corresponding to (111), (200), (220), and (311) in biomass-associated AuNPs. Alternatively, only a single prominent peak was observed at  $2\theta$  angle: 38.22 with a Bragg reflection corresponding to (111) in extracellular AuNPs. Our present findings are consistent with earlier studies that used biological methods to synthesize AuNPs using plant extracts (Chelly et al. 2021a, 2021b), yeast (Krishnan et al. 2021; Krishnan and Chadha 2021) and bacteria (Kalimuthu et al. 2020; Kalishwaralal et al. 2009;

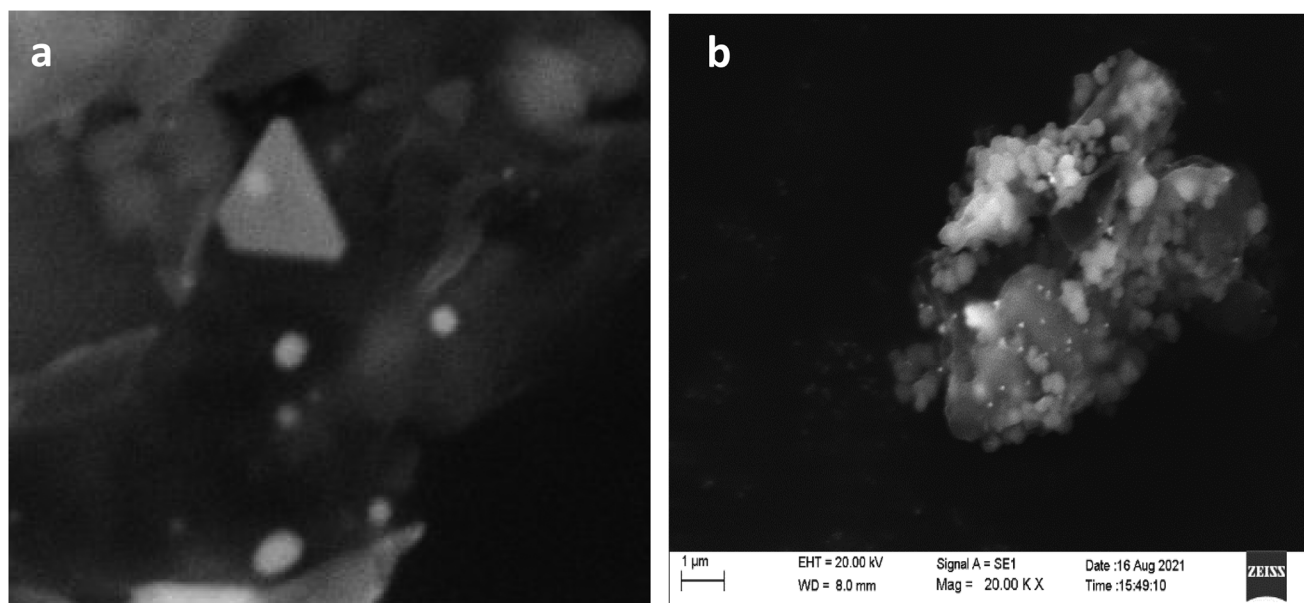


**Figure 7.** (a,b). SEM micrographs of AuNPs in the form of different shapes, such as spheres, hexagons, triangles, rhomboids, and rectangular; polydisperse AuNPs.

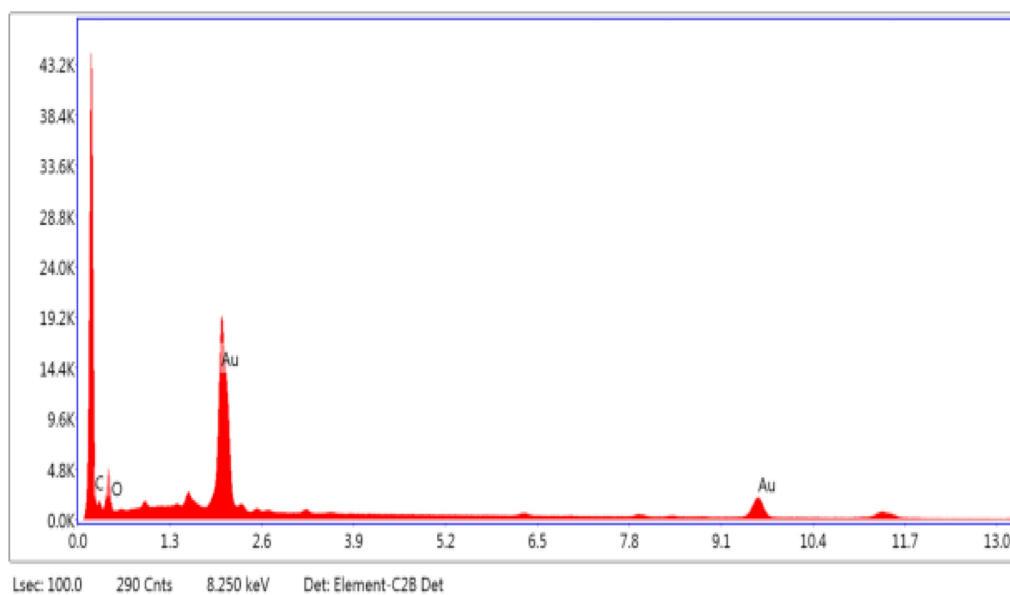


**Figure 8.** EDX of the mycosynthesized AuNPs.

Sathiyaraj et al. 2021). The synthesized materials were investigated by FT-IR spectroscopy to identify the formation of AuNPs and the possible biomolecules involved. The study was done in the range  $4000\text{--}400\text{ cm}^{-1}$ . All samples produced identical spectrum with a slight shift in the band positions. Chemically significant regions of FTIR called spectral windows were identified which included fatty acid region dominated by C–H ( $3450\text{--}2850\text{ cm}^{-1}$ ); amide region dominated by C=O amide I and N–H amide II bands of proteins and peptides ( $1800\text{--}1500\text{ cm}^{-1}$ ); Mixed region ( $1500\text{--}1200\text{ cm}^{-1}$ ); polysaccharides region ( $1200\text{--}900\text{ cm}^{-1}$ ); true finger-printing region ( $900\text{--}700\text{ cm}^{-1}$ ) similar findings are reported earlier (Das et al. 2010a, 2010b). As clearly observed in the spectrum, several absorption peaks were centered at 607, 1073, 1299, 1392, 1547, 1632, 2925, and  $3271\text{ cm}^{-1}$ . Proteins can bind to AuNPs

either through free amine groups or cysteine residues (Dhillon et al. 2012). Thus, the FT-IR data analysis indicates the formation of AuNPs NPs and the presence of protein molecules in the pellets which is responsible for the binding of AuNPs (Sanghi and Verma 2009). Potential of FTIR spectroscopy in chemical characterization of *Termitomyces heimii* pellets has been carried out earlier where similar finding are reported (D'Souza and Kamat 2009). It is well known that surface enhanced Raman signal is proportional to the Raman cross section of the adsorbed molecule, the excitation laser intensity, and the number of molecules that are involved in the SERS process. SERS effect occurs because of the very strong electromagnetic fields and field gradients available in the so-called 'hot spots' of the colloidal cluster. Therefore, the molecules involved in the SERS effect are pre-dominantly

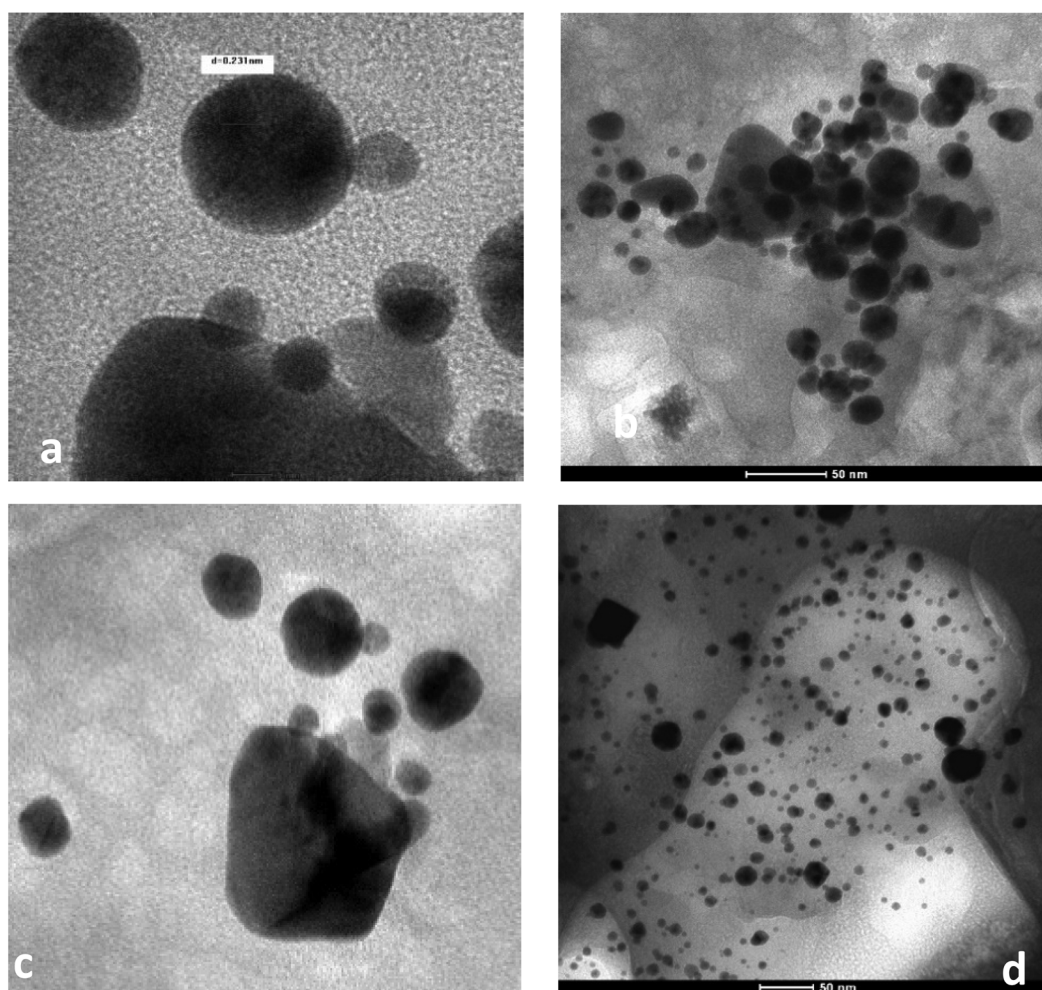


**Figure 9.** (a–d). TEM microphotographs of AuNPs of different shapes synthesized by *Termitomyces heimii* pellet.

those adsorbed on aggregates that have favorable SPRs. Scientist have studied aggregated NPs which have additional plasmon resonances, associated with inter-particle plasmon coupling. They showed that longer wavelength, inter particle plasmon resonances of NP aggregates provide an even better excitation frequency for SERS (Zhao et al. 2019). The peak obtained at  $1326.23$ ,  $1338.99$ ,  $1356$ , and  $1363.52\text{ cm}^{-1}$  were due to  $\delta\text{CH}_2$  (wag),  $\delta\text{CH}_2$  (twist), and  $\nu\text{C}$  single bond N modes, respectively. Peak obtained at  $1556.16$  is due to  $\nu(\text{C}(\text{NO}_2))$ ,  $1577.87\text{ cm}^{-1}$  due to  $\nu(\text{N}=\text{N})$  aliphatic. Presently mostly used techniques and available for characterization and direct size determination are TEM and SEM. However, because both are solid state (i.e., *ex situ*) techniques, the GNP samples must be taken out of solution, deposited on copper grids (for TEM) or other solid support (for SEM) and dried before the analysis which means that further NP growth in the increasingly concentrated solution cannot be prevented.

SEM micrographs of AuNPs in the form of different shapes such as spheres, hexagons, triangles, rhomboids, and rectangular. NPs with varied morphologies have been reported in previous study (Philip 2009; Sen et al. 2013). SEM demonstrated a polymorphic distribution in size and shapes of AuNPs. Maximum NPs were in the range of 20–50 nm. Few NPs were in the range of 50–150 and 150–500 nm. SEM attached with SEM-EDX is an analytical

technique that is used for the elemental analysis or chemical characterization. In this study, for verification of AuNPs, EDX spectroscopy analysis was carried out to confirm that the presence of elemental Au was confirmed by signals. The energy dispersive spectroscopic analysis is done to get an indication of the amount of AuNPs present in the biomass. EDS analysis of thin film of fungal biomass shows strong signals for Gold atoms. Figure 4 shows presence of Gold which is the AuNPs. The specific EDX analysis of the residue resulting from the interaction of the fungus extract with the Gold salt. This indicates the presence of the Gold component, which comes from AuNPs (Owaid et al. 2017). Generally, Figure 8 also shows the presence of carbon, Nitrogen, and oxygen, due to the various organic compounds such as amino acids, fatty acids, and polyphenols present in the mushroom (Javed et al. 2019; Yang et al. 2017). TEM analysis was conducted to evaluate the shape and microstructure of the synthesized AuNPs. A typical TEM image of the synthesized AuNPs is shown in Figure 7(a–d). As clearly observed, the synthesized NPs were well dispersed with spherical structures. In fact, spherical NPs were more abundant than NPs of other shapes. This spherical shape indicated that the synthesized NPs had minimum surface energy and high thermodynamic stability, which confirmed the high value of the zeta potential of the synthesized AuNPs. The

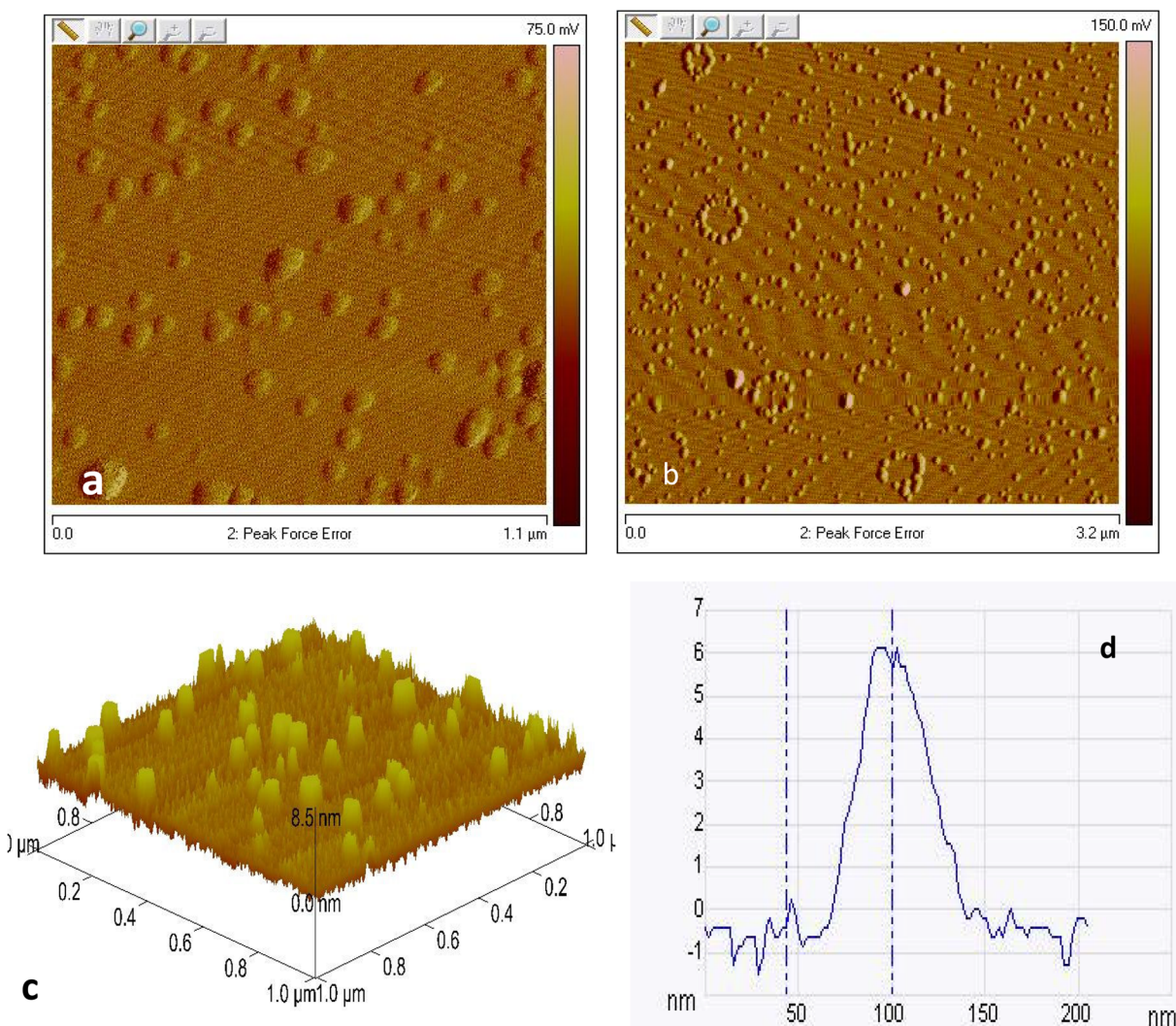


**Figure 10.** (a–d): a) AFM images of the AuNPs, b) distinguishable small AuNPs, c) 3D-image of Gold nanoclusters at the mica surface, and d) the histograms of the normalized number of AuNPs.

obtained results were in agreement with the finding of Bhat et al. (2013). They indicated that the edible mushroom *Termitomyces* pellets can be used to biosynthesize spherical AuNPs with the particle size ranging from 10 to 50 nm. The TEM images showed a successful synthesis of triangular nano prisms to nearly spherical and hexagonal with different sizes between 20 and 150 nm. The produced NPs were 23.2 nm in size and were mostly spherical in shape. TEM analysis was conducted to evaluate the shape and microstructure of the synthesized AuNPs. As clearly observed, the synthesized they indicated that the edible mushroom *P. florida* extract could be used to biosynthesize spherical AuNPs with the particle size ranging from 10 to 50 nm.

AFM of the protein-capped AuNPs synthesized from *Termitomyces heimii* was illustrated the morphology and roughness in the 2D and 3D topographical graphics (Figure 10). Also, this figure declared the formation of clear geometrical shapes in the AuNPs layer.

Earlier studies were on isolation, identification, cultivation, and determination of antimicrobial  $\beta$ -glucan from a wild-termite mushroom *Termitomyces heimii* RFES 230662 (Ahmad et al. 2021). Highly selective and sensitive

colorimetric detection of arsenic (III) in aqueous solution using green synthesized unmodified gold NPs has been reported earlier (Harisha et al. 2023). Potential of FTIR spectroscopy in chemical characterization of *Termitomyces* Pellets has been carried out earlier where similar finding are reported (D'Souza and Kamat 2009). Application of digital colorimeter for preliminary characterization of AuNPs swarms produced by *Termitomyces heimii* extracts using a novel bioinspired microfluidics assay (Dabolkar and Kamat 2020). A colorimetric optical sensor for detection of  $Hg^{2+}$  ions in aqueous solution has been developed using silver NPs (Harisha et al. 2019; Sanjeevappa et al. 2022). This is the first report on use of *Termitomyces heimii* pellets for the synthesis of AuNPs and its characterization in Goa and India. The process of AuNPs synthesis and characterization is shown in Figure 11.

## Conclusions

This research is considered the first attempt to mycosynthesize AuNPs from the *Termitomyces heimii* pellets, and their characterization. Present research results showed that the color change of the mixture from light yellow to purple after

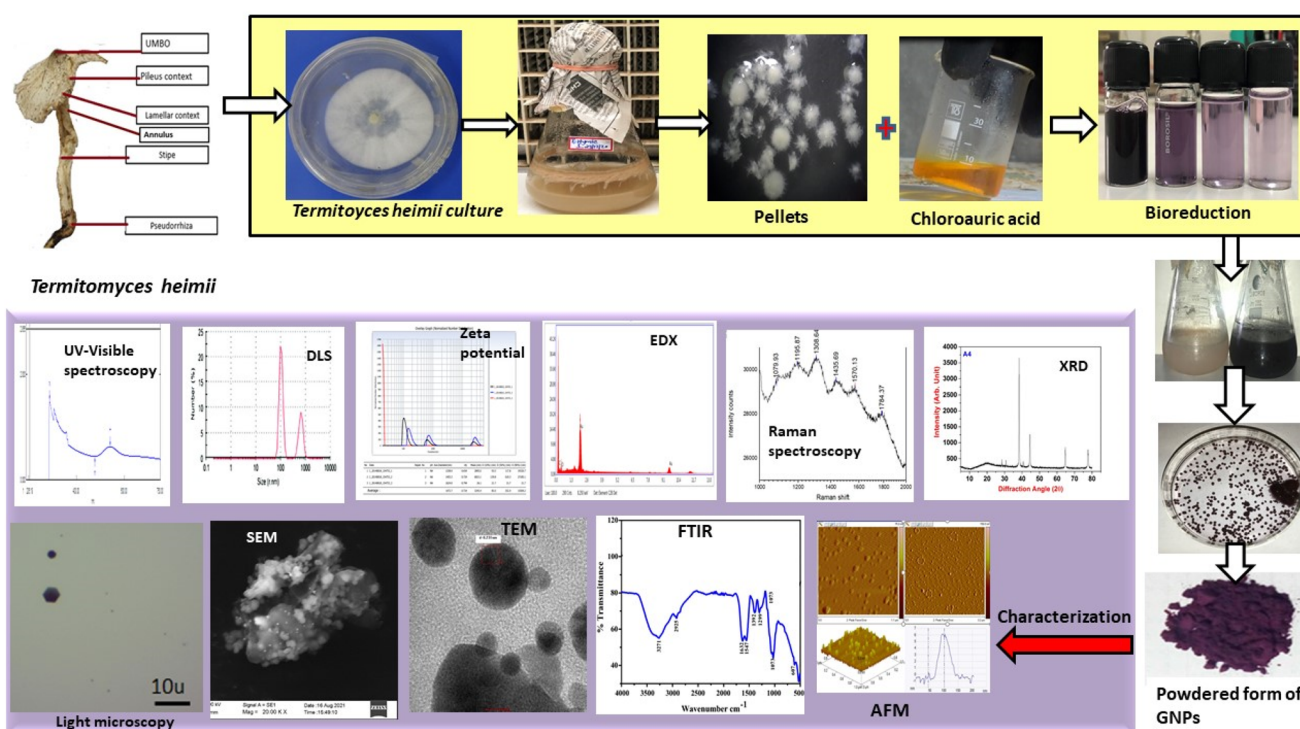


**Figure 11.** The mycosynthesis and characterization of AuNPs using *Termitomyces heimii* pellets.

25 min and the lambda max of the absorbance reached 530 nm using the UV-visible spectrum, which is evidence of the formation of AuNPs from the pellets. The FTIR spectra revealed active groups like carbonyl group (C=O) and a hydroxyl group (-OH), belonging to the peptides, proteins, flavonoids, monosaccharides, polysaccharides, and phenolic compounds. The EDX technique showed that the formed NPs were AuNPs with C, H, N, and S elements due to the amino acid composition and the organic matter of the mushroom. XRD results showed that AuNPs have a face-centered cubic (fcc) crystal. This mushroom-mediated green chemistry approach toward the synthesis of AuNPs has many advantages like ease with the process can be scaled up and economic viability. As mushroom is rich in proteins, there is increased productivity of NPs compared to other biosynthesis routes already reported. Apart from being environmentally benign, there is a key advantage in using mushroom extract as reducing agent. *Termitomyces heimii* being the most dominant species in Goa and state mushroom of Goa was used for the present investigations. It can be grown on large scale in form of pellets and can be useful at large scale production of AuNPs. This process can be carried out at the industrial scale for mass production of AuNPs in future studies.

### Acknowledgments

Ms. Sujata Dabolkar acknowledges UGC, NF-OBC Junior Research Fellowship. Thanks are due to Dr. Absar Ahmad, Director, Interdisciplinary Center for Nanotechnology AMU for guidance.

### Disclosure statement

The authors report no conflicts of interest. The authors are responsible for the content and writing of this article.

### Funding

This work was supported by Goa University Fungus Culture Collection (GUFCC) and University Grants Commission.

### ORCID

Sujata Dabolkar  <http://orcid.org/0000-0001-6141-3069>

Nandkumar M. Kamat  <http://orcid.org/0000-0003-1070-0492>

### References

- Abdul-Hadi SY, Owaid MN, Rabeea MA, Aziz AA, Jameel MS. 2020. Rapid mycosynthesis and characterization of phenols-capped crystal AuNPs from *Ganoderma applanatum*, Ganodermataceae. *Biocatal Agric Biotechnol* 27:101683.
- Acay H. 2021. Utilization of *Morchella esculenta*-mediated green synthesis Golden nanoparticles in biomedicine applications. *Prep Biochem Biotechnol* 51(2):127–136.
- Ahmad A, Senapati S, Khan MI, Kumar R, Sastry M. 2003. Extracellular biosynthesis of monodisperse AuNPs by a novel extremophilic actinomycete, *Thermomonospora* sp. *Langmuir* 19(8):3550–3553.
- Ahmad A, Senapati S, Khan MI, Kumar R, Sastry M. 2005. Extra-/intra-cellular biosynthesis of AuNPs by an alkalotolerant fungus, *Trichothecium* sp. *J Biomed Nanotechnol* 1(1):47–53.
- Ahmad R, Sellathore S, Ngadi E, Saharuddin TST, Zakaria II, Selvakumaran S, Wan WAAQI. 2021. Isolation, identification, cultivation and determination of antimicrobial  $\beta$ -glucan from a wild-termite mushroom *Termitomyces heimii* RFES 230662. *Biocatal Agric Biotechnol* 37:102187.
- Bae AH, Numata M, Yamada S, Shinkai S. 2007. New approach to preparing one-dimensional Au nanowires utilizing a helical structure constructed by schizophyllan. *New J Chem* 31(5):618–622.
- Banerjee K, Ravishankar Rai V. 2018. A review on mycosynthesis, mechanism, and characterization of silver and AuNPs. *BioNanoSci* 8(1):17–31.
- Barabadi H, Honary S, Ebrahimi P, Mohammadi MA, Alizadeh A, Naghibi F. 2014. Microbial Mediated Preparation, Characterization and Optimization of AuNPs. Available at [www.sbmicrobiologia.org.br](http://www.sbmicrobiologia.org.br).

- Basiev TT, Sobol AA, Zverev PG, Osiko VV, Powell RC. 1999. Comparative spontaneous Raman spectroscopy of crystals for Raman lasers. *Appl Opt* 38(3):594–598.
- Bhat R, Sharanabasava VG, Deshpande R, Shetti U, Sanjeev G, Venkataraman A. 2013. Photo-bio-synthesis of irregular shaped functionalized AuNPs using edible mushroom *Pleurotus florida* and its anticancer evaluation. *J Photochem Photobiol B* 125:63–69.
- Bhattarai B, Zaker Y, Bigioni TP. 2018. Green synthesis of gold and silver nanoparticles: challenges and opportunities. *Curr Opin Green Sustain Chem* 12:91–100.
- Botha WJ, Eicker A. 1991. Cultural studies on the genus *Termitomyces* in South Africa. I. Macro-and microscopic characters of basidiome context cultures. *Mycol Res* 95(4):435–443.
- Chelly M, Chelly S, Zribi R, Bouaziz-Ketata H, Gdoura R, Lavanya N, Veerapandi G, Sekar C, Neri G. 2021a. Synthesis of silver and AuNPs from *Rumex roseus* plant extract and their application in electrochemical sensors. *Nanomaterials* 11(3):739.
- Chelly S, Chelly M, Zribi R, Gdoura R, Bouaziz-Ketata H, Neri G. 2021b. Electrochemical detection of dopamine and riboflavine on a screen-printed carbon electrode modified by AuNPs derived from *Rhizoglyphus nigellus* plant extract. *ACS Omega* 6(37):23666–23675.
- Dabolkar S, Kamat NM. 2020. Application of digital colorimeter for preliminary characterization of Gold nanoparticle swarms produced by *Termitomyces heimii* using a novel bioinspired microfluidics assay. *Kavaka* 55:50–57.
- Das RK, Borthakur BB, Bora U. 2010a. Green synthesis of AuNPs using ethanolic leaf extract of *Centella asiatica*. *Mater Lett* 64(13):1445–1447.
- Das SK, Das AR, Guha AK. 2010b. Microbial synthesis of multishaped Gold nanostructures. *Small* 6(9):1012–1021.
- De Souza RA, Kamat NM. 2018. Evaluation and characterization of pellet morphology of genus *Termitomyces heimii* of a wild tropical edible mushroom. *J Pharm Chem Biol Sci* 6(4):320–328.
- De Souza RA, Kamat NM, Nadkarni VS. 2018. Purification and characterisation of a sulphur rich melanin from edible mushroom *Termitomyces albuminosus* Heim. *Mycology* 9(4):296–306.
- Dheyab MA, Owaid MN, Rabeea MA, Aziz AA, Jameel MS. 2020. Mycosynthesis of AuNPs by the Portabella mushroom extract, Agaricaceae, and their efficacy for decolorization of Azo dye. *Environ Nanotechnol Monitor Manag* 14:100312.
- Dhillon GS, Brar SK, Kaur S, Verma M. 2012. Green approach for nanoparticle biosynthesis by fungi: current trends and applications. *Crit Rev Biotechnol* 32(1):49–73.
- D'Souza RA, Kamat NM. 2009. Potential of FTIR spectroscopy in chemical characterization of *Termitomyces* pellets. *J Appl Biol Biotechnol* 5(04):080–084.
- El-Batal AI, ElKenawy NM, Yassin AS, Amin MA. 2015. Laccase production by *Pleurotus ostreatus* and its application in synthesis of AuNPs. *Biotechnol Rep (Amst)* 5:31–39.
- Eskandari-Nojehdehi M, Jafarizadeh-Malmiri H, Rahbar-Shahrouzi J. 2018. Hydrothermal green synthesis of AuNPs using mushroom (*Agaricus bisporus*) extract: physico-chemical characteristics and antifungal activity studies. *Green Proc Synth* 7(1):38–47.
- Falconer DM, Craw D, Youngson JH, Faure K. 2006. Gold and sulphide minerals in Tertiary quartz pebble conglomerate Gold placers, Southland, New Zealand. *Ore Geol Rev* 28(4):525–545.
- Ganesan K, Jothi VK, Natarajan A, Rajaram A, Ravichandran S, Ramalingam S. 2020. Green synthesis of Copper oxide nanoparticles decorated with graphene oxide for anticancer activity and catalytic applications. *Arabian J Chem* 13(8):6802–6814.
- Gour A, Jain NK. 2019. Advances in green synthesis of nanoparticles. *Artif Cells Nanomed Biotechnol* 47(1):844–851.
- Harisha KS, Narayana B, Sangappa Y. 2023. Highly selective and sensitive colorimetric detection of arsenic (III) in aqueous solution using green synthesized unmodified gold nanoparticles. *J Dispersion Sci Technol* 44(1):132–143.
- Harisha KS, Shilpa M, Asha S, Parushuram N, Ranjana R, Narayana B, Sangappa Y. 2019. Synthesis of silver nanoparticles using *Bombyx mori* silk fibroin and antibacterial activity. *IOP Conf Ser Mater Sci Eng* 577(1):012008.
- Heim R. 1977. Termites and Fungi; Termitophilic Fungi from Black Africa and Southern Asia, Societe Nouvelle des Eds. Paris: Boubee. ISBN 2850040045.1-207
- Heim R. 1942. New descriptive studies on *Termitophilic Agarics* from tropical Africa. *Arch Mus Natl Hist Nat Paris* 6:1–133.
- Hendra PJ, Stratton PM. 1969. Laser-Raman spectroscopy. *Chem Rev* 69(3):325–344.
- Herizchi R, Abbasi E, Milani M, Akbarzadeh A. 2016. Current methods for synthesis of AuNPs. *Artif Cells Nanomed Biotechnol* 44(2):596–602.
- Javed I, Peng G, Xing Y, Yu T, Zhao M, Kakinen A, Faridi A, Parish CL, Ding F, Davis TP, et al. 2019. Inhibition of amyloid beta toxicity in zebrafish with a chaperone-Gold nanoparticle dual strategy. *Nat Commun* 10(1):3780.
- Ji Y, Cao Y, Song Y. 2019. Green synthesis of AuNPs using a *Cordyceps militaris* extract and their antiproliferative effect in liver cancer cells (HepG2). *Artif Cells Nanomed Biotechnol* 47(1):2737–2745.
- Kalimuthu K, Cha BS, Kim S, Park KS. 2020. Eco-friendly synthesis and biomedical applications of AuNPs: a review. *Microchem J* 152:104296.
- Kalishwaralal K, Deepak V, Pandian SRK, Gurunathan S. 2009. Biological synthesis of Gold nanocubes from *Bacillus licheniformis*. *Bioresour Technol* 100(21):5356–5358.
- Kalisz HM, Wood DA, Moore D. 1986. Regulation of extracellular laccase production of *Agaricus bisporus* by nitrogen sources in the medium. *FEMS Microbiol Lett* 34(1):65–68.
- Karun NC, Sridhar KR. 2013. Occurrence and distribution of *Termitomyces* (Basidiomycota, Agaricales) in the Western Ghats and on the west coast of India. *Czech Mycol* 65(2):233–254.
- Katas H, Lim CS, Azlan AYHN, Buang F, Busra MFM. 2019. Antibacterial activity of biosynthesized AuNPs using biomolecules from *Lignosus rhinocerotis* and chitosan. *Saudi Pharm J* 27(2):283–292.
- Krishnan S, Chadha A. 2021. Microbial synthesis of AuNPs and their applications as catalysts. *Handbook of Nanomaterials and Nanocomposites for Energy and Environmental Applications*. Berlin, Germany: Springer, p. 1081–1108.
- Krishnan S, Patel PN, Balasubramanian KK, Chadha A. 2021. Yeast supported AuNPs: an efficient catalyst for the synthesis of commercially important aryl amines. *New J Chem* 45(4):1915–1923.
- Lee SO, Kim MJ, Kim DG, Choi HJ. 2005. Antioxidative activities of temperature-stepwise water extracts from *Inonotus obliquus*. *J Korean Soc Food Sci Nutr* 34(2):139–147.
- Long DA. 1977. *Raman Spectroscopy*. New York, NY: McGraw-Hill.
- Morris B. 1986. Notes on the genus *Termitomyces* Heim in Malawi. *Soc Malawi J* 39(1):40–49.
- Mossebo DC, Njounkou AL, Piatek M, Kengni B, Diasbe MD. 2009. *Termitomyces striatus* f. *pileatus* f. nov. and f. *brunneus* f. nov. from Cameroon with a key to central African species. *Mycotaxon* 107(1):315–329.
- Nadeem M, Abbasi BH, Younas M, Ahmad W, Khan T. 2017. A review of the green syntheses and anti-microbial applications of AuNPs. *Green Chem Lett Rev* 10(4):216–227.
- Naem GA, Jaloot AS, Owaid MN, Muslim RF. 2021. Green synthesis of AuNPs from *Coprinus comatus*, agaricaceae, and the effect of ultraviolet irradiation on their characteristics. *Walailak J Sci Tech* 18(8):9312–9396.
- Narayanan KB, Park HH, Han, SS. 2015. Synthesis and characterization of biomatrixed-AuNPs by the mushroom *Flammulina velutipes* and its heterogeneous catalytic potential. *Chemosphere* 141:169–175.
- Natarajan K. 1979. South Indian Agaricales V: *Termitomyces heimii*. *Mycologia* 71(4):853–855.
- Owaid MN, Al-Saedi SSS, Abed IA. 2017. Biosynthesis of AuNPs using yellow oyster mushroom *Pleurotus cornucopiae* var. *citrinopileatus*. *Environ Nanotechnol Monitor Manag* 8:157–162.
- Owaid MN, Rabeea MA, Aziz AA, Jameel MS, Dheyab MA. 2019. Mushroom-assisted synthesis of triangle AuNPs using the aqueous extract of fresh *Lentinula edodes* (shiitake), Omphalotaceae. *Environ Nanotechnol Monitor Manag* 12:100270.
- Singh P, Kim Y, Yang D. 2016. A strategic approach for rapid synthesis of Gold and silver nanoparticles by Panax ginseng leaves. *Artif Cell Nanomed* 44:1949–1957.

- Pegler DN, Vanhaecke M. 1994. *Termitomyces* of southeast Asia. *Kew Bull* 49(4):717–736.
- Philip D. 2009. Biosynthesis of Au, Ag and Au–Ag nanoparticles using edible mushroom extract. *Spectrochim Acta A Mol Biomol Spectrosc* 73(2):374–381.
- Rabaea MA, Owaid MN, Aziz AA, Jameel MS, Dheyab MA. 2020. Mycosynthesis of AuNPs using the extract of *Flammulina velutipes*, Physalacriaceae, and their efficacy for decolorization of methylene blue. *J Environ Chem Eng* 8(3):103841.
- Raman J, Hariprasath Lakshmanan PAJ, Zhijian C, Periasamy V, David P, Naidu M, Sabaratnam V. 2015. Neurite outgrowth stimulatory effects of myco synthesized AuNPs from *Hericium erinaceus* (Bull.: Fr.) Pers. on pheochromocytoma (Pc-12) cells. *Int J Nanomed* 10:5853.
- Sanghi R, Verma P. 2009. Biomimetic synthesis and characterisation of protein capped silver nanoparticles. *Bioresour Technol* 100(1):501–504.
- Sanjeevappa HK, Nilogal P, Rayaraddy R, Martis LJ, Osman SM, Badiadka N, Yallappa S. 2022. Biosynthesized unmodified silver nanoparticles: a colorimetric optical sensor for detection of Hg<sup>2+</sup> ions in aqueous solution. *Result Chem.* 4:100507.
- Sarkar J, Roy SK, Laskar A, Chattopadhyay D, Acharya K. 2013. Bioreduction of chloroaurate ions to AuNPs by culture filtrate of *Pleurotus sapidus* Quel. *Mater Lett.* 92:313–316.
- Sathiyaraj S, Suriyakala G, Gandhi AD, Babujanathanam R, Almaary KS, Chen TW, Kaviyarasu K. 2021. Biosynthesis, characterization, and antibacterial activity of AuNPs. *J Infect Public Health.* 14(12):1842–1847.
- Savitzky A, Golay MJ. 1964. Smoothing and differentiation of data by simplified least squares procedures. *Anal Chem* 36(8):1627–1639.
- Sen IK, Maity K, Islam SS. 2013. Green synthesis of AuNPs using a glucan of an edible mushroom and study of catalytic activity. *Carbohydr Polym* 91(2):518–528.
- Stamets P, Chilton JS. 1983. *The Mushroom Cultivator*. Kent, WA: First Washington.
- Syed A, Al Saedi MH, Bahkali AH, Elgorgan AM, Kharat M, Pai K, Ahmad A. 2020. αAu<sub>2</sub>S nanoparticles: Fungal-mediated synthesis, structural characterization and bioassay. *Green Chem Lett Rev* 15(1):59–68.
- Teimuri-Mofrad R, Hadi R, Tahmasebi B, Farhoudian S, Mehravar M, Nasiri R. 2017. Green synthesis of AuNPs using plant extract: Mini-review. *Nanochem Res* 2(1):8–19.
- Tepale N, Fernández-Escamilla VVA, Carreon-Alvarez C, González-Coronel VJ, Luna-Flores A, Carreon-Alvarez A, Aguilar J. 2019. Nanoengineering of AuNPs: green synthesis, characterization, and applications. *Crystals* 9(12):612.
- Tibuhwa DD. 2012. *Termitomyces* species from Tanzania, their cultural properties and unequalled basidiospores. *JBLs* 3(1):140–159.
- Tibuhwa DD, Kivaisi AK, Magingo FSS. 2010. Utility of the macro-micromorphological characteristics used in classifying the species of *Termitomyces*. *Tanzania J Sci* 36(1):31–45.
- Tsutsui Y, Hayakawa T, Kawamura G, Nogami M. 2011. Tuned longitudinal surface plasmon resonance and third-order nonlinear optical properties of Gold nanorods. *Nanotechnology* 22(27):275203.
- Tudu SC, Zubko M, Kusz J, Bhattacharjee A. 2021. CdS nanoparticles (< 5 nm): green synthesized using *Termitomyces heimii* mushroom—structural, optical and morphological studies. *Appl Phys A* 127(2):1–9.
- Usman AI, Aziz AA, Noqta OA. 2017. Application of green synthesis of AuNPs: a review. *J Teknol* 79(5):1–5.
- Vetchinkina EP, Loshchinina EA, Burov AM, Nikitina VE. 2013. Bioreduction of Gold (iii) ions from hydrogen tetrachloraurate to the elementary state by edible cultivated medicinal xylophilic Basidiomycetes belonging to various systematic groups and molecular mechanisms of AuNPs biological synthesis. *Sci Pract J Heal Life Sci.* 4:51–56.
- Vetchinkina EP, Loshchinina EA, Vodolazov IR, Kursky VF, Dykman LA, Nikitina VE. 2017. Biosynthesis of nanoparticles of metals and metalloids by basidiomycetes. Preparation of AuNPs by using purified fungal phenol oxidases. *Appl Microbiol Biotechnol* 101(3):1047–1062.
- Vrinda KB, Pradeep CK. 2009. *Termitomyces sagittiformis*-a lesser known edible mushroom from the Western Ghats. *Mushroom Res* 18(1):33–36.
- Wei TZ, Tang BH, Yao YJ. 2009. Revision of *Termitomyces* in China. *Mycotaxon* 108(1):257–285.
- Yang G, Nanda J, Wang B, Chen G, Hallinan DT, Jr. 2017. Self-assembly of large AuNPs for surface-enhanced Raman spectroscopy. *ACS Appl Mater Interfaces* 9(15):13457–13470.
- Zhao Y, Zhao W, Lim YC, Liu T. 2019. Salinomycin-loaded AuNPs for treating cancer stem cells by ferroptosis-induced cell death. *Mol Pharm* 16(6):2532–2539.